



# Stabilization of sphingomyelin interactions by interfacial hydroxyls – A study of phytosphingomyelin properties

Shishir Jaikishan, J. Peter Slotte \*

Biochemistry, Department of Biosciences, Åbo Akademi University, Tykistökatu 6A, 20520 Turku, Finland

## ARTICLE INFO

### Article history:

Received 3 July 2012

Received in revised form 27 August 2012

Accepted 30 August 2012

Available online 7 September 2012

### Keywords:

Cholesterol

Sphingolipids

Cholestatrienol

Fluorescence quenching

Anisotropy

DSC

## ABSTRACT

*D-ribo*-phytosphingosines are biologically significant long-chain bases present in various sphingolipids from yeasts, fungi, plants and mammals. In this study we prepared phytopalmitoylsphingomyelin (phytoPSM) analogs based on the *D-ribo*-phytosphingosine base. The *N*-linked acyl chains were either 16:0, 2OH(R)16:0 (natural isomer), or 2OH(S)16:0. The gel-phase of phytoPSM was more stable than that of PSM ( $T_m$  48.6 °C and 41.0 °C, respectively). The gel-liquid crystalline phase transition enthalpies were  $9.1 \pm 0.4$  and  $6.1 \pm 0.3$  kcal/mol for phytoPSM and PSM, respectively. An *N*-linked 2OH(R)16:0 in phytoPSM destabilized the gel phase relative to phytoPSM (by  $\sim +6$  °C, based on DPH anisotropy measurements), whereas 2OH(S)16:0 in phytoPSM stabilized it (by  $\sim -6$  °C). All phytoPSM analogs formed sterol-enriched ordered domains in a fluid ternary bilayer, and those containing phytoPSM or 2OH(S)phytoPSM were more thermostable than the domains containing 2OH(R)phytoPSM or PSM. The affinity of cholestatrienol for POPC bilayers containing 20 mol% phytoPSM was higher than for comparable bilayers with an equal amount of PSM. The 2-hydroxylated acyl chains in phytoPSM did not markedly alter sterol affinity. We conclude that phytoPSM is a more ordered sphingolipid than PSM, and is fully capable of interacting with cholesterol.

© 2012 Elsevier B.V. All rights reserved.

## 1. Introduction

Sphingolipids constitute a group of very important lipid components in eukaryotic cell membranes. Sphingolipids can be distinguished from other membrane lipid species by the long-chain base, which most often is either sphingosine (18:1<sup>Δ4t</sup>), dihydrosphingosine (18:0), or phytosphingosine [1–3]. Modifications of the basic structure of the long-chain base, the head group, or the *N*-linked acyl chains lead to a huge number of different molecular species of sphingolipids which are present in various cells and tissues. This variation in structure, and thus function, help cells in performing many specific and different functions in e.g., cell recognition, in heat stress responses and cell signaling [2,3].

Phytosphingosine (*D-ribo*-1,3,4-trihydroxy-2-aminooctadecane) is a long chain natural sphingolipid possessing an additional hydroxyl group at C-4 position of sphingosine, thus also lacking the trans double bond at C-4 [4]. Phytosphingosine is a sphingolipid occurring naturally both in its free form and as a part of the major fraction of ceramides. Phytosphingosines were first identified in glycosphingolipids isolated from plants by Carter and collaborators [4] and subsequently found in

yeasts, protozoa, sea urchins, amoebae, fish as well as mammalian kidney, intestine and adenocarcinoma cells [5–9]. Recently, sphingomyelin (SM) molecular species, in which the long-chain base is phytosphingosine, was found in significant amounts in human breast milk as well as in bovine milk [10,11]. In addition to having hydroxylated long-chain bases, sphingolipids also incorporate  $\alpha$ -hydroxylated fatty acids in their *N*-linked position [12]. Hydroxylated sphingolipids have important biological effects in cells and tissues. For example,  $\alpha$ -hydroxylated cerobrosides are important for the stability of the myelin sheet [12]. Hydroxylated ceramides (both in the long-chain base and in the acyl chain) exist abundantly in the skin where they together with cholesterol, cholesterol sulfate, and fatty acids help to maintain the barrier function of skin [13]. The presence of  $\alpha$ -hydroxylation in cerobroside sulphates stabilizes intermolecular interactions, and increase gel/liquid crystalline phase transition temperatures in hydrated model membrane systems [14,15]. Membrane stabilization by a 2OH(R)-fatty acid in galactosylceramide bilayers has also been reported [16]. Hydroxyl-related stabilization of molecular packing is seen with ceramide monolayers, where  $\alpha$ -hydroxylated ceramides are more condensed compared to their nonhydroxylated counterparts [17]. We showed recently that  $\alpha$ -hydroxylated SM has a much more stable gel phase as compared to non-hydroxylated SM [18]. The affinity of cholesterol to bilayers containing  $\alpha$ -hydroxylated SM was less than observed for bilayers containing non-hydroxylated SM species [18].

Since very few biophysical studies exist in which the effects of the long-chain base hydroxylation have been studied, we have undertaken to study how SM properties change when an additional hydroxyl is

**Abbreviations:** 7SLPC, 1-palmitoyl-2-stearoyl-(7-doxyl)-sn-glycero-3-phosphocholine; CTL, cholesta-5,7,9 (11)-trien-3- $\beta$ -ol; DPH, 1,6-diphenyl-1,3,5-hexatriene;  $K_m$ , partitioning coefficient; POPC, 1-palmitoyl-2-oleoyl-sn-glycero-3-phosphocholine; SM, sphingomyelin;  $T_m$ , mid temperature of the gel to liquid-crystalline phase transition;  $T_{1/2}$ , half-width of the gel to liquid-crystalline phase transition

\* Corresponding author. Tel.: +358 2 2154 689; fax: +358 2 2410 014.

E-mail address: [jpslotte@abo.fi](mailto:jpslotte@abo.fi) (J.P. Slotte).

incorporated in the 4-position of the long-chain base, yielding phytosphingomyelin (Scheme 1). We selected to study SM instead of e.g., cerebrosides, since its preparation was more feasible, it is physiologically relevant, and since the biophysical properties of various structural SM analogs have been studied extensively by us and by others.

## 2. Materials and methods

Highly pure 1-palmitoyl-2-oleoyl-*sn*-glycero-3-phosphocholine (POPC) and D-erythro-phytosphingosyl phosphorylcholine were purchased from Avanti Polar Lipids (Alabaster, AL, USA) and used without further purification.  $\alpha$ -Hydroxylated palmitic acid used for SM synthesis were obtained from Larodan Fine Chemicals (Malmö Sweden). *N*-palmitoyl-*D*-erythro-sphingomyelin (PSM) was purified from egg sphingomyelin using reverse-phase HPLC as described in [19]. The identity of purified PSM was verified by ESI-MS (purity better than 99%). 1-Palmitoyl-2-stearoyl-(7-doxyl)-*sn*-glycero-3-phosphocholine (7SLPC) and cholesta-5,7,9(11)-trienol (CTL) respectively, were synthesized and purified as described previously [20–22]. The identity of CTL was positively verified by APCI-MS. 1,6-Diphenyl-1,3,5-hexatriene (DPH) was purchased from Molecular Probes (Leiden, the Netherlands). The fluorophores were stored under argon in the dark at  $-87^\circ\text{C}$  until dissolved in argon-purged ethanol (CTL) or methanol (DPH). The concentration of CTL and DPH in the respective stock solutions was determined spectrophotometrically using their molar absorption coefficients ( $\epsilon$ ) values:  $11,250\text{ M}^{-1}\text{cm}^{-1}$  at 324 nm for CTL, and  $88,000\text{ M}^{-1}\text{cm}^{-1}$  at 350 nm for DPH. *c*-Laurdan was kindly provided by professor Bong Rae Cho (Department of Chemistry and Center for Electro- and Photo-Responsive Molecules, Korea University 1-Anamdong, Seoul 136–701, Korea) and synthesized as described in reference [23]. Stock solutions of the lipids, prepared in hexane/2-propanol (3/2, by vol) were stored at  $-20^\circ\text{C}$  and used within a week. All the phospholipid stock solutions were taken to ambient temperature before use and the concentration of the lipids was determined by phosphate assay subsequent to total digestion by perchloric acid. Water was used as aqueous solvent in all studies. All other inorganic and organic chemicals used were of the highest purity available. The solvents used were of spectroscopic grade. Water was purified by reverse osmosis followed by passage through a Millipore UF Plus water purification system having final resistivity of  $18.2\text{ M}\Omega\text{ cm}$ .

### 2.1. Synthesis of phytoPSM analogs

PhytoPSM was prepared from phytosphingosyl phosphorylcholine and palmitic anhydride as follows:  $5\text{ }\mu\text{mol}$  of phytosphingosyl phosphorylcholine was reacted with  $15\text{ }\mu\text{mol}$  of palmitic anhydride in  $0.3\text{ ml}$  dry chloroform in the presence of  $5\text{ }\mu\text{l}$  trimethylamine. After 60 min at  $40^\circ\text{C}$ , the reaction volume was reduced to dryness (with nitrogen gas). The synthesis mix was taken up in  $1\text{ ml}$  dry methanol, and purified using preparative HPLC (Supelco Discovery

C18 column, dimension  $250\times 21\text{ mm}$  with  $5\text{ }\mu\text{m}$  particle size) and elution with pure methanol. The phytoPSM fraction was collected, and the identity was verified by ESI-MS analysis.

For the preparation of  $\alpha$ -hydroxylated phytoPSM analogs, the racemic 2(OH)-palmitic acid was first converted to its *N*-hydroxysuccinimide esters, as described previously [24]. Coupling of the activated hydroxyl-fatty acid with sphingosyl phosphorylcholine was performed as described for phytoPSM. Purification of the  $\alpha$ -hydroxylated phytoPSM analogs by preparative HPLC gave two equal fractions eluting 3–4 min apart. Both fractions contained a product with the correct molecular weight (based on the  $\text{M}^+$ -Na adduct  $m/z$  value). We have previously demonstrated that 2OH(S)-containing SM elute after the 2OH(R)-SM analog [18], and assuming that the 4-OH in the long-chain base of phytoPSM did not interfere with elution order, we have assigned the first eluting component as 2OH(R)phytoPSM and the last eluting component as 2OH(S)phytoPSM.

### 2.2. Preparation of liposomes

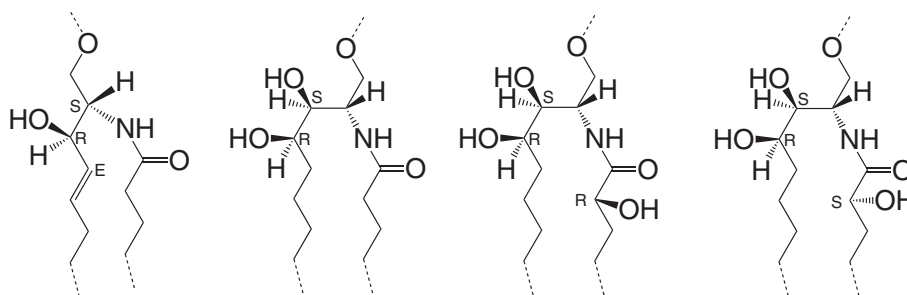
Lipid vesicles were used as model membranes for all experiments in this work. Multilamellar lipid vesicles used in fluorimetric studies were prepared by mixing lipids and probes to a final concentration of  $50\text{ }\mu\text{M}$  (spectroscopy) or  $1.4\text{ mM}$  (calorimetry). Appropriate amounts of the lipids and probes were mixed and the solvent was dried under a constant stream of  $\text{N}_2$  at  $40^\circ\text{C}$  to yield an apparently homogenous lipid film. The lipid film was further dried in the high vacuum for at least 1–2 h at room temperature. Lipid films were hydrated by adding warm milliQ water for 20 min at a temperature above  $T_m$  of the highest melting lipid. The lipids were dispersed by vigorous mixing (Vortex). Vesicles for spectroscopy were additionally sonicated for 2 min using a W-450 Branson Ultrasonics probe sonicator (20% duty cycle, 15 W power setting). Vesicles for equilibrium partitioning were extruded (11x) through  $200\text{ nm}$  filters at a temperature above the  $T_m$  of the highest melting lipid.

### 2.3. DSC measurements

Differential scanning calorimetry was performed with a VP-DSC instrument (MicroCal, Northampton/MA, USA) to obtain the  $T_m$  and  $\Delta H$  for the main transition of some SM analog bilayers, and to obtain information about mutual interactions in bilayer membranes, essentially as described previously [25].

### 2.4. Determination of steady state fluorescence anisotropy

Steady-state anisotropy of 1,6-diphenyl-3,5-hexatriene (DPH) was measured to obtain acyl chain order information for pure SM analog bilayers, and for SM bilayers containing increasing amounts of cholesterol, essentially as described previously [19]. The wave lengths of excitation and emission of DPH were  $360\text{ nm}$  and  $430\text{ nm}$ , respectively. The steady state anisotropy was calculated as described in [26].



**Scheme 1.** Molecular structure of phytoSM analogs studied. From left to right: PSM, phytoPSM, 2OH(R)phytoPSM, 2OH(S)phytoPSM.

## 2.5. Determination of *c*-laurdan fluorescence

The emission spectra of *c*-laurdan were determined for pure SM analog bilayers in the gel or liquid-crystalline phase, to obtain information about interfacial hydration and lateral packing properties, as described previously [27]. The temperature for analysis was selected to be  $-5\text{ }^{\circ}\text{C}$  or  $+5\text{ }^{\circ}\text{C}$  from the  $T_m$  for each SM analog. Each experimental temperature is indicated in the figure legend. The total lipid concentration in the assay was  $50\text{ }\mu\text{M}$  and the *c*-laurdan concentration was 1 mol%. Excitation was at 365 nm and emission spectra were recorded between 390 and 550 nm.

## 2.6. Fluorescence quenching measurements

In order to follow the formation and melting of ordered domains, the steady-state quenching of CTL by the quencher 7 SLPC was measured on a PTI QuantaMaster spectrofluorimeter (Photon Technology International, Lawrenceville, NJ, USA). The excitation and the emission slits were set to 5 nm and the temperature was controlled by a Peltier element with a temperature probe immersed in the sample solution. The samples were heated from  $7\text{ }^{\circ}\text{C}$  to  $70\text{ }^{\circ}\text{C}$  at a rate of  $5\text{ }^{\circ}\text{C}/\text{min}$ . The measurements were done in quartz cuvettes with a light path length of 1 cm and the sample solutions were kept at a constant stirring (350 rpm) throughout the fluorescence measurement. Fluorescence intensity of CTL was detected with excitation and emission wavelengths at 324 nm and 374 nm. The fluorescent probe was protected from light during all the steps of experiments. Fluorescence emission intensity was measured in the F-sample (quenched) consisting of POPC/7SLPC/SM analog/cholesterol, (30:30:30:10, molar ratio) and in the  $F_0$  sample (non-quenched), in which 7SLPC had been replaced with POPC [28]. The fluorescence intensity in the F sample was divided by the fluorescence intensity of the  $F_0$  sample giving the fraction of non-quenched CTL fluorescence plotted versus the temperature. CTL replaced 1 mol% of cholesterol and was added to the lipid solution prior to drying.

## 2.7. CTL equilibrium partitioning between unilamellar vesicles and cyclodextrin

The partitioning of CTL between large unilamellar vesicles and methyl- $\beta$ -cyclodextrin (m $\beta$ CD; Sigma chemicals, St. Louis, MO) was measured to determine the affinity of the sterol for the bilayers containing SM analogs [29,30]. The partitioning coefficient was calculated as described previously [29,30]. The assay yields the molar fraction partition coefficient,  $K_x$ , for CTL. The CTL and thus sterol concentration was 2 mol% in all partitioning experiments.

## 3. Results

### 3.1. Properties of pure phytoPSM bilayers

Since *N*-acyl chain hydroxylated SMs showed marked stabilization of the gel phase, we have made phytoPSM, which has an additional hydroxyl group in the long-chain base, and tested whether this hydroxyl function also affects gel phase stability and interlipid cohesion. In addition, we also examined the properties of phytoPSM with  $\alpha$ -hydroxy acyl chains. DSC analysis of pure PSM bilayers is known to give a  $T_m$  of about  $41\text{ }^{\circ}\text{C}$ , and an enthalpy of about 6–7 kcal/mol [31,32]. We confirmed these values for PSM ( $T_m$   $41.0\text{ }^{\circ}\text{C}$ ,  $\Delta H$   $6.1 \pm 0.3$  kcal/mol; Table 1). With pure phytoPSM bilayers, the gel phase was observed to be markedly stabilized by the additional 4-OH in the long-chain base of phytoPSM, since the DSC reported  $T_m$  was  $48.6\text{ }^{\circ}\text{C}$  ( $\Delta H$   $9.1 \pm 0.4$  kcal/mol; Table 1). Binary mixed bilayers containing both PSM and phytoPSM showed a fairly cooperative gel/liquid crystalline phase transition, since the peak width at half height was very similar for PSM and for a 1:1 mixture of PSM and phytoPSM (0.97 and  $0.95\text{ }^{\circ}\text{C}$ , respectively, Table 1). Pure PSM and phytoPSM

**Table 1**

Thermodynamic data for the thermal transitions of PSM analogs derived from DSC analysis of pure or binary bilayer membranes. Thermodynamic data for dihydroPSM is included for comparison.

Lipids	Pretransition	Main transition		
	T ( $^{\circ}\text{C}$ )	$T_m$ ( $^{\circ}\text{C}$ )	$\Delta H$ (kcal/mol)	$T_{1/2}$ ( $^{\circ}\text{C}$ )
PSM	30.4	41.0	$6.1 \pm 0.3$	0.97
dihydroPSM <sup>a</sup>	41.5	46.9	8.5	1.10
PhytoPSM	44.6	48.6	$9.1 \pm 0.4$	0.97
PSM:dihydroPSM (50:50) <sup>a</sup>	32.6	43.6	6.7	1.14
PSM:phytoPSM (50:50)	34.6	42.8	6.2	0.95

<sup>a</sup> Data taken from [40].

bilayers had a pre-transition at 30.4 and  $44.6\text{ }^{\circ}\text{C}$ , respectively (Fig. 1). The pre-transition was retained in the 1:1 binary mixture, where it occurred at an intermediate temperature ( $34.6\text{ }^{\circ}\text{C}$ ; Fig. 1), marginally higher than dihydroPSM:PSM mixture (Table 1).

### 3.2. DPH anisotropy and *c*-laurdan emission spectra in pure SM analog bilayers

Next we analyzed acyl chain order in pure SM analog bilayers as a function of temperature, and also included  $\alpha$ -hydroxylated phytoPSM species. Changes in the relative acyl chain order were deduced from the steady-state anisotropy function of DPH. The main transition, which DPH anisotropy also reports (Fig. 2), agrees fairly well with DSC data (Fig. 1) for PSM and phytoPSM. The change in DPH anisotropy during the transition was also very rapid for both PSM and phytoPSM, indicating a cooperative transition which again agrees with the DSC data. The fluid phase acyl chain order for PSM and phytoPSM appeared to be similar at equal temperatures (e.g., at 55 or  $60\text{ }^{\circ}\text{C}$ , Fig. 2). When phytoPSM was acylated with a 2OH-16:0-fatty acid, the  $T_m$  of the main transition differed markedly depending of the stereo-specific orientation of the  $\alpha$ -hydroxy-group. For 2OH(S)phytoPSM, the gel phase was stabilized compared to phytoPSM, whereas with 2OH(R)phytoPSM (natural isomer), it was destabilized (Fig. 2). The main transition appeared to be fairly cooperative for 2OH(R)phytoPSM, whereas it appeared to be more complex when 2OH(S)phytoPSM was analyzed (Fig. 2). The fluid phase acyl chain order appeared to be slightly higher for the  $\alpha$ -hydroxylated phytoSM analogs as compared to the non-hydroxylated analogs.

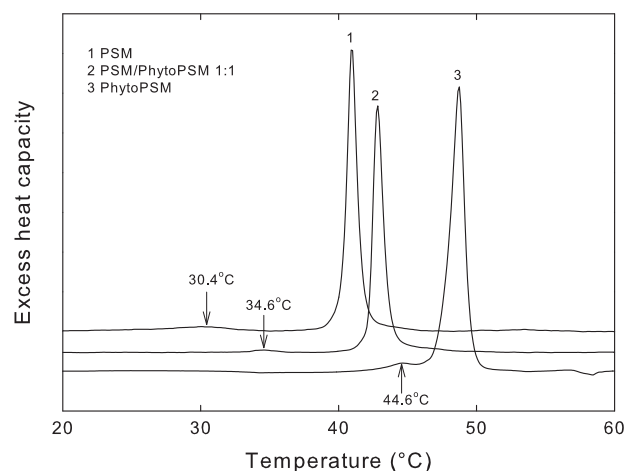


**Fig. 1.** DSC analysis of pure PSM or phytoPSM bilayers. Multilamellar vesicles were prepared to a final phospholipid concentration of 1.4 mM in water. Thermograms of pure PSM or phytoPSM bilayers, or an equimolar mixture of the two, were collected (second heating scan). The temperature gradient was  $1\text{ }^{\circ}\text{C}/\text{min}$ . The pre-transition temperature is indicated.

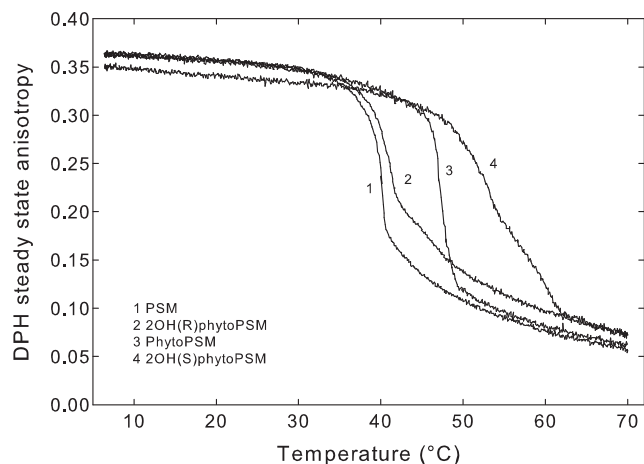


**Fig. 2.** Steady state anisotropy of DPH in pure SM bilayers as a function of temperature. Experiments were performed with multilamellar vesicles (prepared by probe sonication) at a scan rate of 5 °C/min. The samples contained 1 mol% DPH as fluorophore and the lipid concentration was 50  $\mu$ M. The graphs show representative data from reproducible experiments.

In the gel phase, the phytoPSM bilayer interphase appeared to be more hydrated than the PSM bilayer, as indicated by the *c*-laurdan emission shift (Fig. 3A). This difference was abolished in the liquid-disordered phase (Fig. 3B). When phytoPSM contained  $\alpha$ -hydroxylated acyl chains, the gel-phase *c*-laurdan emission shift was even more redshifted for both (2OH(S)-16:0) and (2OH(R)-16:0) analogs, when compared to PSM (Fig. 3A). In the liquid-crystalline phase, all SM analogs showed very similar *c*-laurdan emission profile (Fig. 3B). Clearly, the long-chain base hydroxylation in phytoPSM affected interfacial hydration (compared to PSM) in the gel phase, and additional acyl chain hydroxylation appeared to further increase the interfacial hydration.

### 3.3. Interaction of cholesterol with phytoPSM

To better understand the interaction between cholesterol and the hydroxylated PSM analogs in more complex membranes, we prepared ternary mixed bilayers containing POPC, PSM analog, and cholesterol (60:30:10 by mol), and examined the formation of sterol-enriched ordered domains by a CTL quenching assay [33]. PhytoPSM analogs included in the study were able to form sterol-enriched ordered domains

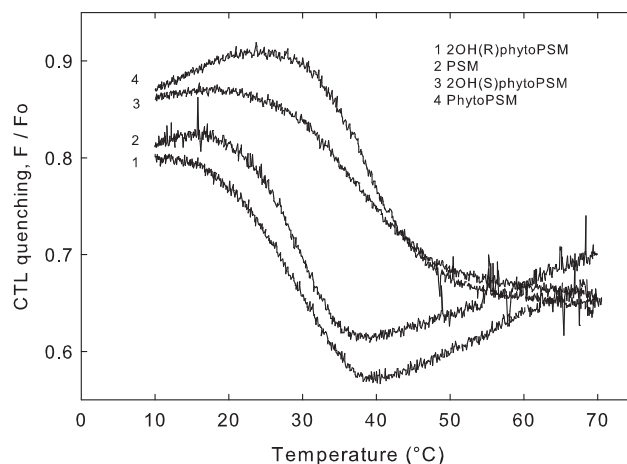


**Fig. 4.** Quenching susceptibility of CTL in ternary bilayer. Multilamellar vesicles prepared by probe sonication were composed of ( $F_0$  sample) POPC/SM analog/cholesterol (60:30:10 by mol). In the  $F$ -sample, 7SLPC replaced half of the POPC. CTL was included at 1 mol%. The melting profile is shown as the  $F/F_0$  ratio plotted versus temperature. Representative curves are shown.

in the fluid POPC bilayers (Fig. 4). The phytoPSM formed more stable ordered domains in comparison to that of PSM (mid melting temperature about 39 °C and 29 °C, respectively, Fig. 4). The stability of ordered domains for  $\alpha$ -hydroxylated phytoPSM analogs, varied depending on the orientation of the  $\alpha$ -hydroxy group, and correlated with the transition temperature of the pure compounds (Fig. 4). With 2OH(R)phytoPSM and 2OH(S)phytoPSM containing domains, the  $T_m$ :s were about 27 and 37 °C, respectively, while the end melting temperatures were about 39 and 49 °C, respectively (Fig. 4). The delta  $F/F_0$  ( $F/F_0$  ratio before and after melting) was similar for all analogs, suggesting that the CTL (and thus sterol) content in the ordered domains were similar for the different SM analog domains.

### 3.4. Sterol affinity for SM analog containing bilayers

A recently developed CTL equilibrium partition assay has been used to further analyze the interaction between cholesterol/CTL and the phytoPSM analogs. We determined the CTL molar fraction equilibrium partition coefficient for POPC bilayers containing 20 mol% of one of the PSM analogs. PSM in POPC bilayers has been shown to

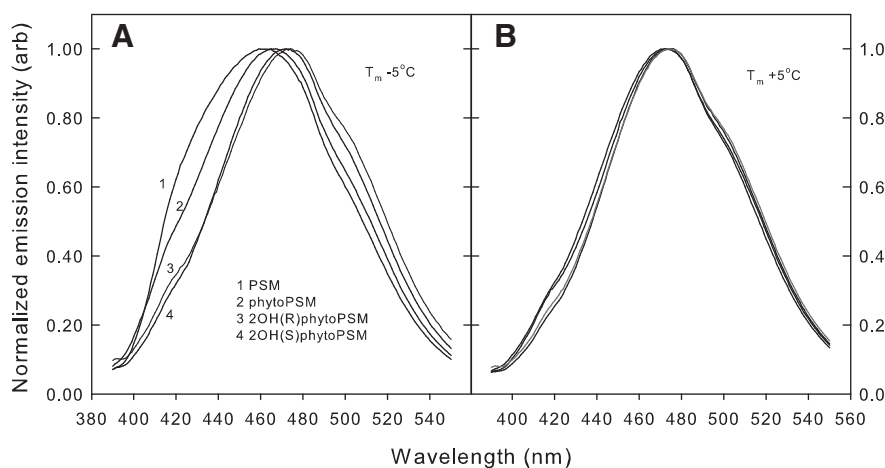


**Fig. 3.** *c*-Laurdan emission spectra from multilamellar vesicles containing PSM, phytoPSM, phytoPSM(2OH-R), or phytoPSM(2OH-S). The total lipid concentration in the assay was 50  $\mu$ M and the *c*-laurdan concentration was 0.1 mol%. Excitation was at 365 nm and emission spectra were recorded between 390 and 550 nm. Panel A shows data obtained from the gel phase at  $T_m$  minus 5 °C, which corresponds to 36 °C for PSM, 42 °C for phytoPSM, 37 °C for 2OH(R)phytoPSM, or 50 °C for 2OH(S)phytoPSM. Panel B shows data obtained from the liquid-crystalline phase at  $T_m$  plus 5 °C, which corresponds to 46 °C for PSM, 52 °C for phytoPSM, 47 °C for 2OH(R)phytoPSM, or 60 °C for 2OH(S)phytoPSM.

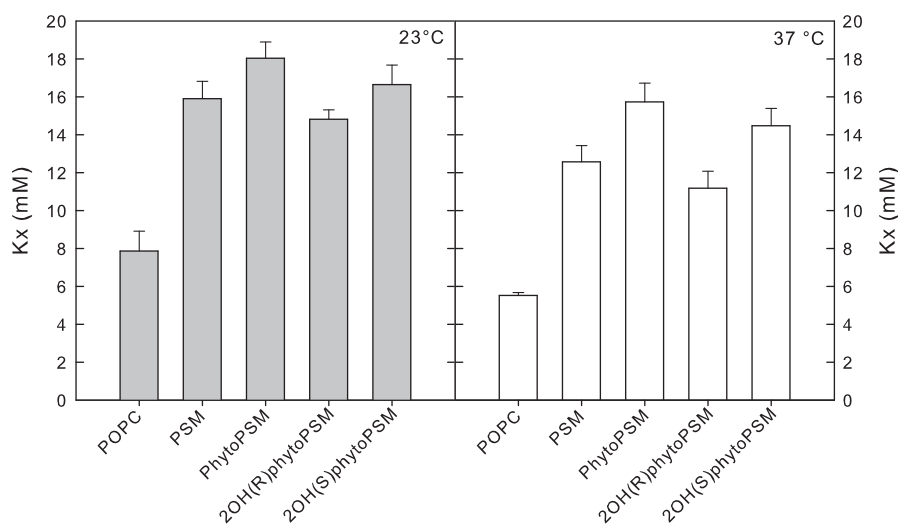


**Fig. 5.** Affinity of CTL for bilayer membranes containing SM analogs in POPC. The equilibrium distribution of CTL between m $\beta$ CD and unilamellar vesicles (prepared by extrusion) was analyzed, and the partitioning coefficient calculated, as described under Methods. The bilayers contained 80 mol% POPC and 20 mol% of one of the SM analogs. The CTL concentration was 2 mol%. A higher  $K_x$  indicates a higher affinity of CTL for the bilayer.

increase the sterol affinity markedly [25,29,34,35], and this was again observed both at 23 and 37 °C (Fig. 5). The CTL affinity for POPC bilayers containing phytoPSM was higher than for bilayers with PSM (both at 23 and 37 °C, Fig. 5), signifying that the additional hydroxyl group in the long-chain base was able to enhance sterol/SM interaction. CTL displayed a high affinity also for  $\alpha$ -hydroxy-phytoPSM containing POPC bilayers than pure POPC bilayers. These affinity results show a good agreement with the CTL quenching data (Fig. 4), which suggested that the ordered domains contained similar amounts of sterol, irrespective of the type of phytoPSM analog used.

#### 4. Discussion

An important feature of sphingolipids is the rather high degree of hydroxylation in the long chain bases (3OH and 4OH) and in the *N*-linked acyl chains (2OH) [36]. Hydroxylated (3OH or 4OH) long chain bases have been shown to be of importance for many biological processes, for example in cell wall formation and asexual/sexual growth in *Aspergillus nidulans* [37]. In mammals, hydroxylated (4OH) long chain bases are minor yet important components of sphingolipids. The interfacial hydroxyl groups have been shown to stabilize the interlipid interactions in model membranes [38,39] but biophysical implications of an additional hydroxyl group (4OH) in long chain base of SM has not been determined. We were interested to study how the phytosphingosine backbone (and  $\alpha$ -hydroxylation simultaneously) in SM affected its membrane properties. Our main objective was to gather information about the interactions between phytoSM and cholesterol to evaluate how the presence of phytosphingosine long chain base in SMs affect the lateral interactions with co-lipids in the membranes. We also examined how additional interfacial hydroxyls in the *N*-linked acyl chains affected phytoPSM properties.

Based on both DSC analysis and DPH steady-state anisotropy, it was evident that the gel-phase was markedly stabilized in phytoPSM bilayers as compared to PSM (Figs. 1 and 2, Table 1). The structural difference between phytoPSM and PSM is the 4-OH in the long-chain base, and the lack of a *trans*  $\Delta^4$  double bond in the long-chain base. It is known that the *trans*  $\Delta^4$  double bond affects gel-phase stability, since dihydro PSM has significantly higher  $T_m$  compared to PSM (Table 1 and [40]). PhytoPSM, which also lacks the  $\Delta^4$  *trans* double bond in the long-chain base, had gel/liquid crystalline phase transition temperature that was 7.6 °C higher than that of PSM (Table 1). The enthalpy value of pure phytoSM bilayers was increased by 3 kcal/mol as compared to PSM bilayers. The enthalpy of the

dihydroSM transition was about 8.5 kcal/mol [40], which is intermediate between those of PSM and phytoPSM. Both the higher  $T_m$  and enthalpy of phytoPSM bilayers, compared to both PSM and dihydroPSM bilayers, suggest that the 4-OH of the long-chain base in phytoPSM was capable of stabilizing gel-phase interactions significantly.

Inclusion of  $\alpha$ -hydroxylated acyl chains in the phytoPSM analog resulted in mixed phase transition behavior depending upon the spatial orientation of the  $\alpha$ -hydroxyl group. 2OH(R)PhytoPSM bilayers showed significantly destabilized gel phases (by DPH anisotropy) when compared to phytoPSM bilayers, whereas 2OH(S)phytoPSM bilayers had significantly increased gel phase stability. If we compare these data with results obtained in a previous study with PSM and  $\alpha$ -hydroxylated PSM, it is evident that  $\alpha$ -hydroxylation in PSM stabilized the gel phase slightly [41] whereas  $\alpha$ -hydroxylation in phytoPSM caused marked destabilization (with the natural  $\alpha$ -hydroxy (R) isomer). Clearly, the  $\alpha$ -hydroxyl in phytoPSM interfered with the gel-phase stabilization caused by the 4-hydroxyl. It is unclear at this moment whether the effect arose from competing hydrogen-bonding (between  $\alpha$ -hydroxyl and 4-hydroxyl) or came from steric packing effects caused by the two opposite hydroxyls in the interfacial region of the molecules. It is also possible that the observed effects were in part related to altered head group dynamics and orientation, since the SM head group is known to interact (at least) with the 3-OH in the long-chain base [42]. Atomistic molecular dynamics simulations of hydroxylated SM bilayers could perhaps provide some information to help explain the cause of these phenomena.

To study how well cholesterol could interact with the hydroxylated PSM analogs, and form ordered sterol-enriched domains, we used a CTL quenching assay (Fig. 5) to elucidate this. Formation of sterol-enriched ordered domains have been demonstrated in ternary bilayers constituting POPC as fluid lipid, PSM as saturated lipid and cholesterol [33]. At low temperatures, CTL present in the ordered domains is more likely to be protected from the collision induced quenching by 7SLPC, present dominantly in fluid glycerophospholipid, POPC. 7SLPC is unlikely to be present in SM rich domains because partitioning of bulky doxyl group is excluded into gel-like phase of saturated long chain SMs. CTL becomes more susceptible to quenching by 7SLPC due to melting of ordered domains with the increase in temperature. We found that all phytoPSM analogs were able to form sterol-enriched ordered domains, and the thermal stability of the domains correlated rather well with the  $T_m$  of the pure PSM analogs (Figs. 4 and 2). It also appeared that the cholesterol/CTL content of the domains (difference in  $F/F_0$  before

and after melting of domains) was rather similar for all compounds. These results suggest that 4-OH in phytoPSM did not adversely affect interactions with cholesterol, and also appeared to increase the stability of such SM/sterol domains in the POPC environment. Surprisingly, an  $\alpha$ -hydroxyl in phytoPSM did not weaken interactions with cholesterol, contrary to results obtained with  $\alpha$ -hydroxylated PSM analogs [41]. This finding clearly suggests that 4-OH directly, or via indirect effects on e.g., acyl chain order, affected cholesterol interaction beneficially.

To further understand the interaction of cholesterol with the phytoSM analogs we used CTL partition [43], an assay significantly modified in our lab from the procedure reported by Niu and Litman [44]. Partitioning data for CTL also correlated with the results obtained by CTL quenching. The CTL affinity was lowest for the POPC bilayers and was higher for all POPC bilayer which contained 20 mol% phytoPSM analogs. Among SM analogs, CTL had the highest affinity for the phytoPSM bilayers. We have shown that CTL affinity for hydroxylated (2OH and 3OH) SM bilayers is lower than PSM [41]. The 2-hydroxylated acyl chains in phytoPSM did not markedly alter sterol affinity yet CTL affinity for 2OH(S)phytoPSM bilayer was higher than that of 2OH(R)phytoPSM.

There have been many studies on the importance of phytosphingosines in physiological processes, both in plants and mammalian cells. We now show that the phytosphingosine backbone in SM is also structurally important for membrane properties of the SM analog. By some yet undetermined mechanism, 4-OH in the long chain base was able to optimize interlipid interactions, not only between SMs but also between SMs and cholesterol. These favorable interactions led to gel phase stabilization, and probably increased cohesiveness between the SM molecules in the fluid phase. The high affinity of cholesterol for phytoPSM can be understood by their increased order parameter, but the role of hydrogen bonding to SM-sterol interaction cannot be excluded as also being important.

## Acknowledgments

We appreciate valuable discussions with Prof. Ilpo Vattulainen regarding this project. This study was supported by generous grants from the Sigrid Juselius Foundation (JPS), the foundation of Åbo Akademi University (SJ), the National Doctoral Program in Informational and Structural Biology (SJ), the Magnus Ehrnrooth Foundation (SJ) and the Oskar Öflunds Foundation (SJ).

## References

- [1] A.H. Merrill Jr., E.M. Schmelz, D.L. Dillehay, S. Spiegel, J.A. Shayman, J.J. Schroeder, R.T. Riley, K.A. Voss, E. Wang, Sphingolipids – the enigmatic lipid class: biochemistry, physiology, and pathophysiology, *Toxicol. Appl. Pharmacol.* 142 (1997) 208–225.
- [2] A.H. Merrill, Y.A. Hannun, R.M. Bell, Introduction: Sphingolipids and Their Metabolites in Cell Regulation, *Advances in Lipid Research* 25 (1993) 1–24.
- [3] A.H. Merrill, C.C. Sweeley, Sphingolipids: Metabolism and Cell Signalling, in: D.E.V.a., E. Vance (Ed.), *Biochemistry of Lipids, Lipoproteins and Membranes*, Elsevier, Science, New York, 1996, pp. 309–339.
- [4] H.E. Carter, H.S. HENDRICKSON, Biochemistry of the sphingolipids. XV. Structure of phytosphingosine and dehydrophytosphingosine, *Biochemistry* 2 (1963) 389–393.
- [5] M.W. Crossman, C.B. Hirschberg, Biosynthesis of phytosphingosine by the rat, *J. Biol. Chem.* 252 (1977) 5815–5819.
- [6] R.C. Dickson, E.E. Nagiec, M. Skrzypek, P. Tillman, G.B. Wells, R.L. Lester, Sphingolipids are potential heat stress signals in *Saccharomyces*, *J. Biol. Chem.* 272 (1997) 30196–30200.
- [7] G.M. Jenkins, A. Richards, T. Wahl, C. Mao, L. Obeid, Y. Hannun, Involvement of yeast sphingolipids in the heat stress response of *Saccharomyces cerevisiae*, *J. Biol. Chem.* 272 (1997) 32566–32572.
- [8] B. Roder, J. Dabrowski, U. Dabrowski, H. Egge, J. Peter-Katalinic, G. Schwarzmann, K. Sandhoff, The determination of phytosphingosine-containing globotriaosylceramide from human kidney in the presence of lactosylceramide, *Chem. Phys. Lipids* 53 (1990) 85–89.
- [9] K. Takamatsu, Phytosphingosine-containing neutral glycosphingolipids and sulfatides in the human female genital tract: their association in the cervical epithelium and the uterine endometrium and their dissociation in the mucosa of fallopian tube with the menstrual cycle, *Keio J. Med.* 41 (1992) 161–167.

- [10] N. Blaas, C. Schuurmann, N. Bartke, B. Stahl, H.U. Humpf, Structural profiling and quantification of sphingomyelin in human breast milk by HPLC-MS/MS, *J. Agric. Food Chem.* 59 (2011) 6018–6024.
- [11] A. Fischbeck, M. Kruger, N. Blaas, H.U. Humpf, Analysis of sphingomyelin in meat based on hydrophilic interaction liquid chromatography coupled to electrospray ionization-tandem mass spectrometry (HILIC-HPLC-ESI-MS/MS), *J. Agric. Food Chem.* 57 (2009) 9469–9474.
- [12] H. Hama, Fatty acid 2-Hydroxylation in mammalian sphingolipid biology, *Biochim. Biophys. Acta* 1801 (2010) 405–414.
- [13] D.T. Downing, Lipid and protein structures in the permeability barrier of mammalian epidermis, *J. Lipid Res.* 33 (1992) 301–313.
- [14] J.M. Boggs, K.M. Koshy, G. Rangaraj, Influence of structural modifications on the phase behavior of semi-synthetic cerebroside sulfate, *Biochim. Biophys. Acta* 938 (1988) 361–372.
- [15] J.M. Boggs, K.M. Koshy, G. Rangaraj, Effect of fatty acid chain length, fatty acid hydroxylation, and various cations on phase behavior of synthetic cerebroside sulfate, *Chem. Phys. Lipids* 36 (1984) 65–89.
- [16] D. Singh, H.C. Jarrell, E. Florio, D.B. Fenske, C.W. Grant, Effects of fatty acid alpha-hydroxylation on glycosphingolipid properties in phosphatidylcholine bilayers, *Biochim. Biophys. Acta* 1103 (1992) 268–274.
- [17] I. Pascher, Molecular arrangements in sphingolipids. Conformation and hydrogen bonding of ceramide and their implication on membrane stability and permeability, *Biochim. Biophys. Acta* 455 (1976) 433–451.
- [18] O. Ekholm, S. Jaikishan, M. Lonnfors, T.K. Nyholm, J.P. Slotte, Membrane bilayer properties of sphingomyelins with amide-linked 2- or 3-hydroxylated fatty acids, *Biochim. Biophys. Acta* 1808 (2011) 727–732.
- [19] S. Jaikishan, A. Bjorkbom, J.P. Slotte, Sphingomyelin analogs with branched N-acyl chains: The position of branching dramatically affects acyl chain order and sterol interactions in bilayer membranes, *Biochim. Biophys. Acta* 1798 (2010) 1987–1994.
- [20] J.T. Mason, A.V. Broccoli, C. Huang, A method for the synthesis of isomerically pure saturated mixed-chain phosphatidylcholines, *Anal. Biochem.* 113 (1981) 96–101.
- [21] S.M. Alanko, K.K. Halling, S. Maunula, J.P. Slotte, B. Ramstedt, Displacement of sterols from sterol/sphingomyelin domains in fluid bilayer membranes by competing molecules, *Biochim. Biophys. Acta* 1715 (2005) 111–121.
- [22] R.T. Fischer, F.A. Stephenson, A. Shafiee, F. Schroeder, delta 5,7,9(11)-Cholestatrien-3 beta-ol: a fluorescent cholesterol analogue, *Chem. Phys. Lipids* 36 (1984) 1–14.
- [23] H.M. Kim, H.J. Choo, S.Y. Jung, Y.G. Ko, W.H. Park, S.J. Jeon, C.H. Kim, T. Joo, B.R. Cho, A two-photon fluorescent probe for lipid raft imaging: C-laurdan, *ChemBioChem* 8 (2007) 553–559.
- [24] Y. Lapidot, S. Rappoport, Y. Wolman, Use of esters of N-hydroxysuccinimide in the synthesis of N-acylamino acids, *J. Lipid Res.* 8 (1967) 142–145.
- [25] C. Sergelius, J.P. Slotte, Membrane properties of and cholesterol's interactions with a biologically relevant three-chain sphingomyelin: 3O-palmitoyl-N-palmitoyl-D-erythro-sphingomyelin, *Biochim. Biophys. Acta* 1808 (2011) 2841–2848.
- [26] J.R. Lakowicz, *Principles of Fluorescence Spectroscopy*, Kluwer Academic / Plenum Publishers, New York, 1999.
- [27] T. Parasassi, E.K. Krasnowska, L. Bagatolli, E. Gratton, LAURDAN and PRODAN as polarity-sensitive fluorescent membrane probes, *J. Fluoresc.* 8 (1998) 365–373.
- [28] S. Jaikishan, A. Bjorkbom, J.P. Slotte, Sphingomyelin analogs with branched N-acyl chains: The position of branching dramatically affects acyl chain order and sterol interactions in bilayer membranes, *Biochim. Biophys. Acta, Biomembr.* 1798 (2010) 1987–1994.
- [29] T.K. Nyholm, P.M. Grandell, B. Westerlund, J.P. Slotte, Sterol affinity for bilayer membranes is affected by their ceramide content and the ceramide chain length, *Biochim. Biophys. Acta* 1798 (2010) 1008–1013.
- [30] J.H. Nystrom, M. Lonnfors, T.K. Nyholm, Transmembrane peptides influence the affinity of sterols for phospholipid bilayers, *Biophys. J.* 99 (2010) 526–533.
- [31] Y. Barenholz, J. Suurkuusk, D. Mountcastle, T.E. Thompson, R.L. Biltonen, A calorimetric study of the thermotropic behavior of aqueous dispersions of natural and synthetic sphingomyelins, *Biochemistry* 15 (1976) 2441–2447.
- [32] P.R. Maulik, G.G. Shipley, N-palmitoyl sphingomyelin bilayers: structure and interactions with cholesterol and dipalmitoylphosphatidylcholine, *Biochemistry* 35 (1996) 8025–8034.
- [33] Y.J. Bjorkqvist, T.K. Nyholm, J.P. Slotte, B. Ramstedt, Domain formation and stability in complex lipid bilayers as reported by cholestatrienol, *Biophys. J.* 88 (2005) 4054–4063.
- [34] S. Jaikishan, J.P. Slotte, Effect of hydrophobic mismatch and interdigitation on sterol/sphingomyelin interaction in ternary bilayer membranes, *Biochim. Biophys. Acta* 1808 (2011) 1940–1945.
- [35] M. Lonnfors, J.P. Doux, J.A. Killian, T.K. Nyholm, J.P. Slotte, Sterols Have Higher Affinity for Sphingomyelin than for Phosphatidylcholine Bilayers even at Equal Acyl-Chain Order, *Biophys. J.* 100 (2011) 2633–2641.
- [36] D.V. Lynch, T.M. Dunn, An introduction to plant sphingolipids and a review of recent advances in understanding their metabolism and function, *New Phytol.* 161 (2004) 677–702.
- [37] S. Li, D. Bao, G. Yuen, S.D. Harris, A.M. Calvo, basA Regulates Cell Wall Organization and Asexual/Sexual Sporulation Ratio in *Aspergillus nidulans*, *Genetics* 176 (2007) 243–253.
- [38] A. Menikh, P.-G. Nyholm, J.M. Boggs, Characterization of the interaction of Ca<sup>2+</sup> with hydroxy and non-hydroxy fatty acid species of cerebroside sulfate by fourier transform infrared spectroscopy and molecular modelling, *Biochemistry* 36 (1997) 3438–3447.
- [39] D. Singh, H.C. Jarrell, E. Florio, D.B. Fenske, C.W.M. Grant, Effects of fatty acid alpha-hydroxylation on glycosphingolipid properties in phosphatidylcholine bilayers, *Biochim. Biophys. Acta, Biomembr.* 1103 (1992) 268–274.

- [40] T.K.M. Nyholm, M. Nylund, J.P. Slotte, A calorimetric study of binary mixtures of dihydrosphingomyelin and sterols, sphingomyelin, or phosphatidylcholine, *Biophys. J.* 84 (2003) 3138–3146.
- [41] O. Ekholm, S. Jaikishan, M. Lonnfors, T.K.M. Nyholm, J.P. Slotte, Membrane bilayer properties of sphingomyelins with amide-linked 2- or 3-hydroxylated fatty acids, *Biochim. Biophys. Acta, Biomembr.* 1808 (2011) 727–732.
- [42] A. Bjorkbom, T. Rog, P. Kankaanpaa, D. Lindroos, K. Kaszuba, M. Kurita, S. Yamaguchi, T. Yamamoto, S. Jaikishan, L. Paavolainen, J. Paivarinne, T.K. Nyholm, S. Katsumura, I. Vattulainen, J.P. Slotte, N- and O-methylation of sphingomyelin markedly affects its membrane properties and interactions with cholesterol, *Biochim. Biophys. Acta* 1808 (2011) 1179–1186.
- [43] T.K. Nyholm, P.M. Grandell, B. Westerlund, J.P. Slotte, Sterol affinity for bilayer membranes is affected by their ceramide content and the ceramide chain length, *Biochim. Biophys. Acta* 1798 (2010) 1008–1013.
- [44] S.L. Niu, B.J. Litman, Determination of membrane cholesterol partition coefficient using a lipid vesicle-cyclodextrin binary system: effect of phospholipid acyl chain unsaturation and headgroup composition, *Biophys. J.* 83 (2002) 3408–3415.